ARL-CR-0762 • MAR 2015

US Army Research Laboratory

Advances in Nanocarbon Metals: Fine Structure

prepared by Lourdes Salamanca-Riba
University of Maryland
1244 Jeong H. Kim Engineering Building
College Park, MD 20742

under contract W911NF-13-1-0058

NOTICES

Disclaimers

The findings in this report are not to be construed as an official Department of the Army position unless so designated by other authorized documents.

Citation of manufacturer's or trade names does not constitute an official endorsement or approval of the use thereof.

Destroy this report when it is no longer needed. Do not return it to the originator.

ARL-CR-0762 ● MAR 2015

US Army Research Laboratory

Advances in Nanocarbon Metals: Fine Structure

prepared by Lourdes Salamanca-Riba
University of Maryland

under contract W911NF-13-1-0058

REPORT DOCUMENTATION PAGE

Form Approved
OMB No. 0704-0188

1. REPORT DATE *(DD-MM-YYYY)*	2. REPORT TYPE	3. DATES COVERED (From - To)
March 2015	Final	March 2013–December 2014

4. TITLE AND SUBTITLE
Advances in Nanocarbon Metals: Fine Structure

5a. CONTRACT NUMBER
W911NF-13-1-0058

5b. GRANT NUMBER

5c. PROGRAM ELEMENT NUMBER

6. AUTHOR(S)
Lourdes Salamanca-Riba

5d. PROJECT NUMBER

5e. TASK NUMBER

5f. WORK UNIT NUMBER

7. PERFORMING ORGANIZATION NAME(S) AND ADDRESS(ES)
University of Maryland
1244 Jeong H. Kim Engineering Building
College Park, MD 20742

8. PERFORMING ORGANIZATION REPORT NUMBER
UMD

9. SPONSORING/MONITORING AGENCY NAME(S) AND ADDRESS(ES)
US Army Research Laboratory
ATTN: RDRL-WMM-F
Aberdeen Proving Ground, MD 21005-5069

10. SPONSOR/MONITOR'S ACRONYM(S)

11. SPONSOR/MONITOR'S REPORT NUMBER(S)
ARL-CR-0762

12. DISTRIBUTION/AVAILABILITY STATEMENT
Approved for public release; distribution is unlimited.

13. SUPPLEMENTARY NOTES

14. ABSTRACT

This study is an investigation of the structure and some properties of silver, copper, and aluminum alloy covetics. Covetics can incorporate large amounts of carbon (C) in a nanoscale form to alter physical and mechanical properties of the base metal or alloy. Once the C has been incorporated into the matrix, it is highly stable and remains dispersed in the material after remelting and resolidification. Characterization of the thin film and bulk covetics was accomplished using X-ray diffraction, Raman spectroscopy, and transmission electron microscopy. Interesting property changes were detected for the different covetic materials. However, the samples always had nonuniformity of the C incorporation. Going forward, it is important to develop a method that will give rise to a more uniform distribution of the C so that a correlation between C content and properties can be obtained.

15. SUBJECT TERMS
covetic, nanocarbon silver, aluminum, copper

16. SECURITY CLASSIFICATION OF:			17. LIMITATION OF ABSTRACT	18. NUMBER OF PAGES	19a. NAME OF RESPONSIBLE PERSON
a. REPORT	b. ABSTRACT	c. THIS PAGE			Kevin Doherty
Unclassified	Unclassified	Unclassified	UU	56	19b. TELEPHONE NUMBER (Include area code) 410-306-0871

Standard Form 298 (Rev. 8/98)
Prescribed by ANSI Std. Z39.18

Contents

INTENTIONALLY LEFT BLANK.

1. Introduction

Recent advances in nanomanufacturing have made it possible for large amounts (>8 wt%) of carbon (C) to be incorporated as nanoscale C during a reaction process in molten aluminum (Al), copper (Cu), silver (Ag), and other elements. These materials, developed by Third Millennium Materials, LLC, are called "covetics".[1] The process of conversion to covetics consists of heating the metal to a temperature above its melting point, adding C in various forms and applying a direct current to the melt while stirring. This process is a relatively simple process that produces a material with many unique and improved properties over the base metal from which it is generated. After the conversion process, the C is highly stable, despite its form not being predicted in phase diagrams, and remains dispersed in the material after remelting and resolidification. The C is bonded to the metal matrix and has an effect on several of the properties of the material.

2. Discussion

In this study we investigated the structure and some properties of Ag, Cu, and Al alloy covetics. We also deposited Cu covetic films by e-beam evaporation and pulsed laser deposition (PLD) and examined the electrical and transmittance properties of Cu covetic films compared with pure Cu films of the same thickness. The bulk samples for this investigation were obtained from Third Millennium Materials, LLC. Pieces of the bulk material were used as targets for the film deposition. The attached PowerPoint presentation (Appendix) given at a meeting at the Defense Advanced Research Projects Agency on 30 September 2014 has more details on the results for the project. The team members with their respective responsibilities are presented on slide 2 of the presentation.

We characterized the structure of the bulk covetics by X-ray diffraction (XRD) and transmission electron microscopy (TEM). No sample showed indications of any of the different allotropes of C by XRD. In TEM, however, we found localized regions of Ag and Al6061 covetics that showed weak spots in the diffraction patterns corresponding to graphitic carbon. These regions not only had crystalline graphitic spots, but also indicated a 3-dimensional epitaxial configuration with the metal host. The epitaxial relationship is $(111)_{Ag\ (Al)}//(0001)_{Graphite}$ and $< 1\bar{1}0 >_{Ag\ (Al)}//< 11\bar{2}0 >_{Graphite}$. Furthermore, both Ag and Al covetics show graphitic modes in their Raman spectra indicating that C in these samples has *sp2* bonding in agreement with the electron diffraction patterns and electron energy loss spectroscopy (EELS) data. Additionally, our discrete Fourier transform (DFT)–based calculations of the phonon density of states in Ag

and Al covetics with layers of graphite reproduced the Raman active modes obtained experimentally not only for the D and G peaks of graphite but also for new weak modes corresponding to Ag-(Al)-C bonding that were obtained in the Raman spectra from Ag and Al covetics. The metal-C bonds form at edges of graphene-like sheets and wherever there is a C vacancy within the graphene layer. DFT indicates bond energy of 1.2-2.2 eV/C atom. More details of the results from Ag and Al covetics can be found, respectively, in slides 5–20 and 21–31 of the Appendix. A paper on Ag covetic is ready for submission to the journal *Advanced Functional Materials*. Another paper on Al covetic is in preparation.

Cu covetic has a different structure than Ag and Al covetics. The XRD spectra from Cu covetic appear just like pure Cu. No evidence for any allotrope of C, CuO, or Cu_2O was found in any of the bulk Cu covetic samples. The electron diffraction patterns in TEM also show no evidence for any of these phases. Instead, weak spots were visible in the diffraction pattern of Cu covetic that correspond to modulations of approximately 1.6 nm along several crystallographic directions of the Cu host lattice that are visible in the images from the areas with the weak spots. The intensity of the weak spots increases with increasing C content in the local region. Results from bulk Cu covetic are presented in slides 32–39 of the Appendix.

Slides 40–56 present analysis of Raman and EELS spectra as indications of *sp2* bonding in covetics. The temperature dependence of the electrical resistivity of Ag covetic is presented in slides 57–59. It is remarkable that the conductivity of Ag covetic with 6-wt% C at room temperature is 90% that of 99.999 Ag. We believe that further improvement in the processing of covetics could give rise to even higher values of the conductivity.

Using pieces of bulk Cu covetic as targets, we deposited films by e-beam evaporation and PLD. Pairs of films were deposited at the same time where one film was deposited on silicon and one on glass substrates for further analysis of the films. For comparison, films of Cu metal (0% C) were also grown using the same conditions. The e-beam deposited films were crystalline with preferred orientation along <111>. The films were continuous with fairly flat surfaces and columnar structure. Cu covetic films deposited on glass were consistently more transparent to light than Cu films of the same thickness, indicating that C incorporation in the films assists in making the film more transparent. Furthermore, the covetic films were also more stable to the environment, as concluded from the smaller changes in resistivity with time in the Cu covetic films compared with the Cu metal films.

Our preliminary results from PLD Cu covetic films showed further improvement in the transmittance of the films compared with the e-beam deposited films, but the films had some problems with C separating from the Cu. The results from the films look very promising, although further attempts to optimize the deposition parameters are necessary to improve the performance and stability of Cu covetic films grown by PLD. Slides 60–81 present our results on Cu covetic films. We have submitted a paper on Cu covetic films for transparent electrodes for publication in the journal *Applied Physics Letters*.

3. Conclusions

In conclusion, we have obtained very interesting results of Ag, Al, and Cu covetics both in bulk and film form. Carbon in covetics changes the properties of the material. However, the samples always had nonuniformity of the C incorporation. It is important to develop a method that will give rise to more uniform distribution of the C so that a correlation between C content and properties can be obtained. Once this is achieved, the properties of covetics could be tuned by the C content and postprocessing conditions. It is also important to investigate what is the maximum C content that can be introduced in the host lattice by this method.

4. Reference

1. Shugart JV, Scherer RC, inventors; Third Millennium Metals, LLC, assignee. Metal-carbon compositions. United States patent US 8,349,759. 2013 Jan 8.

Appendix. Advances in Nanocarbon Materials: Fine Structure Final Report

This appendix appears in its original form, without editorial change.

Advances in Nanocarbon Materials: Fine Structure Final Report

Lourdes Salamanca-Riba
University of Maryland
September 30, 2014

Funded by DARPA/ARL under contract W911NF1310058

Team Members

- Lourdes Salamanca-Riba, MSE University of Maryland
  - Romaine Isaacs (graduate student)
    - Structure and composition analysis of bulk and film covetics
- Liangbing Hu, MSE University of Maryland
  - Hongli Zhu (post-doctoral fellow)
    - Optical and electrical characterization of thin film covetics
- Maija Kukla, MSE University of Maryland
  - Sergey Rashkeev (research fellow)
    - DFT calculations of the structure of covetics

Objectives

- To perform a detailed investigation of the structure and bond-type of Al, Ag and Cu covetic samples that will be obtained from TM^2 and Cu covetic samples received from Carnegie Mellon University.
- To use e-beam deposition and PLD to fabricate Cu covetic films from the Cu covetic bulk samples.
- To use XRD, SEM, EDS, EELS, Raman and AFM to investigate the structure, morphology, composition and bond type of Al and Cu covetics bulk and film.
- To perform Density Functional Theory calculations to obtain the equilibrium structure of covetics.

Outline[&]

Bulk covetics
- Comparison of the structure of bulk Ag, Al alloys and Cu covetics
  - XRD, TEM, SEM, DFT
- Incorporation of C in bulk Ag, Al and Cu covetic
  - Evidence of *sp2* bonding -- Raman, EELS, DFT
- Properties of bulk Ag, Al and Cu covetic
  - electrical measurements of Ag covetic

Film covetics
- E-beam deposition of Cu covetic films
  - Structure
  - Resistivity
  - Transmittance
- PLD deposition of Cu cv films
  - XRD, SEM

[&] All samples in this study were converted to covetics by Third Millennium Materials, LLC.

Structure of Bulk Ag Covetic

Structure of Bulk Ag Covetic

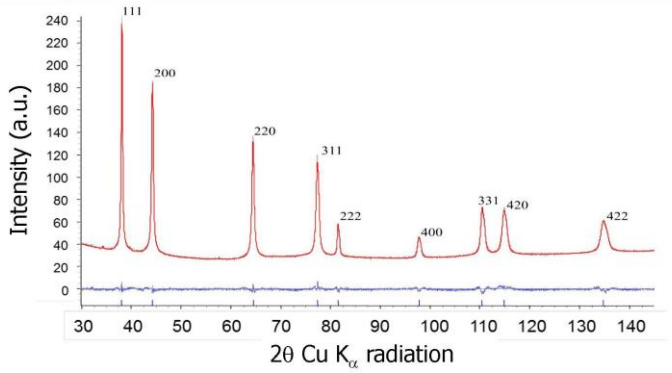

Experimental (blue) and Rietveld fitting (red) from powder Ag cv 6% (36.44 at.%)
Difference (purple) with theoretical positions of the peaks for Ag.

- No peaks for any allotrope of carbon are observed.
- Lattice constant of Ag cv 6% *a*=0.40877(1) nm lattice expansion of~0.05% compared to Ag metal.
- Preferential texture along <111>.

Structure of Ag Covetic at the Nanoscale

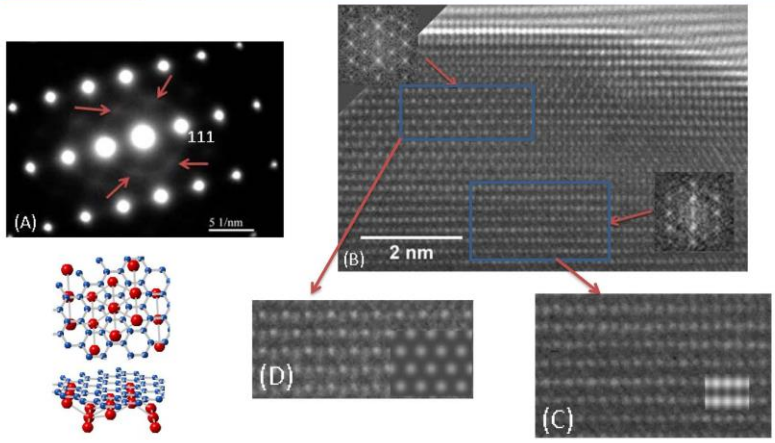

- Strong spots in (A) correspond to $[11\bar{2}]$ zone axis of Ag.
- Weak and broad spots in (A) correspond to $< 2\bar{1}\bar{1}0 >$ spots of graphite
- HRTEM image in (C) and computer image simulation of $[11\bar{2}]$ plane of Ag.
- HRTEM image in (D) and computer image simulation of graphene.

7

Approved for Public Release//Distribution Unlimited.

Ag Covetic at the Nanoscale

Ag cv 3% (21.74 at%)

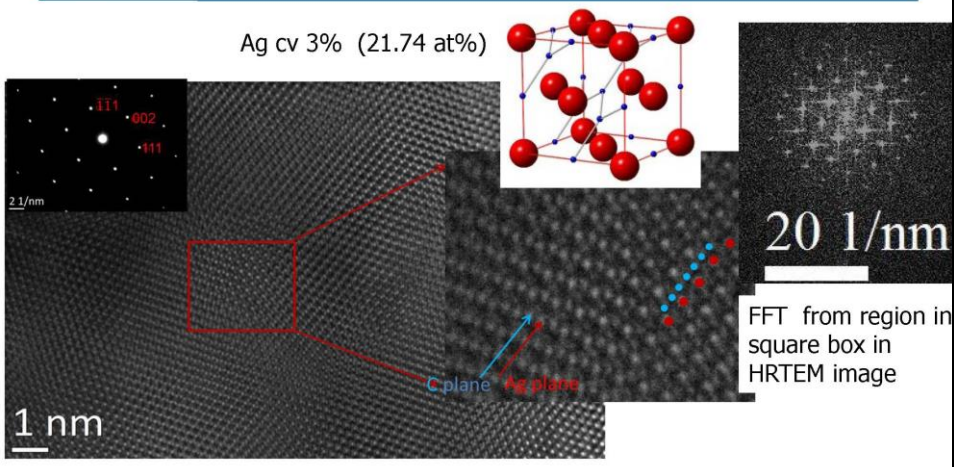

Ag and graphene form alternating layers of (111) plane of Ag and a layer of graphene without disturbing the fcc structure of Ag, i.e., C at interstitial sites.

FFT shows weak spots from graphene-like regions

8

Approved for Public Release//Distribution Unlimited.

IFFT of HRTEM Image of Ag cv 3%

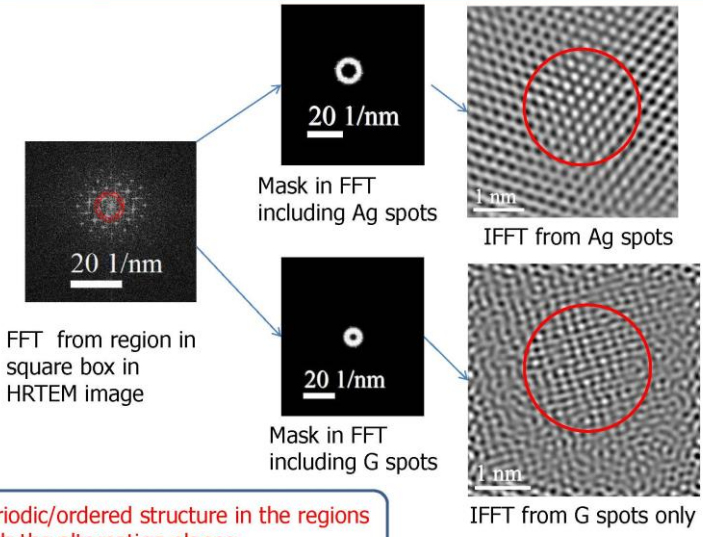

Periodic/ordered structure in the regions with the alternating planes.

9

Approved for Public Release//Distribution Unlimited.

TEM Ag cv 3%

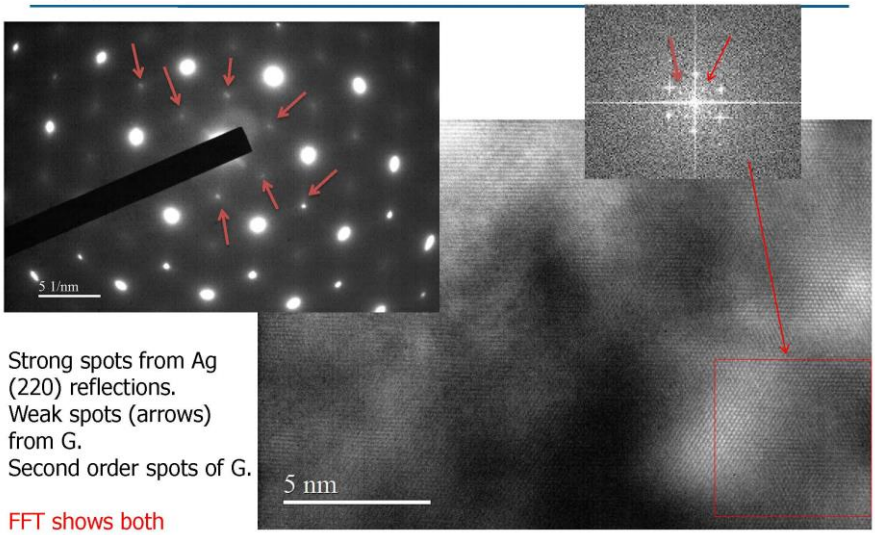

Strong spots from Ag (220) reflections.
Weak spots (arrows) from G.
Second order spots of G.

FFT shows both periodicities.

Approved for Public Release//Distribution Unlimited.

10

(111) Planes of Ag

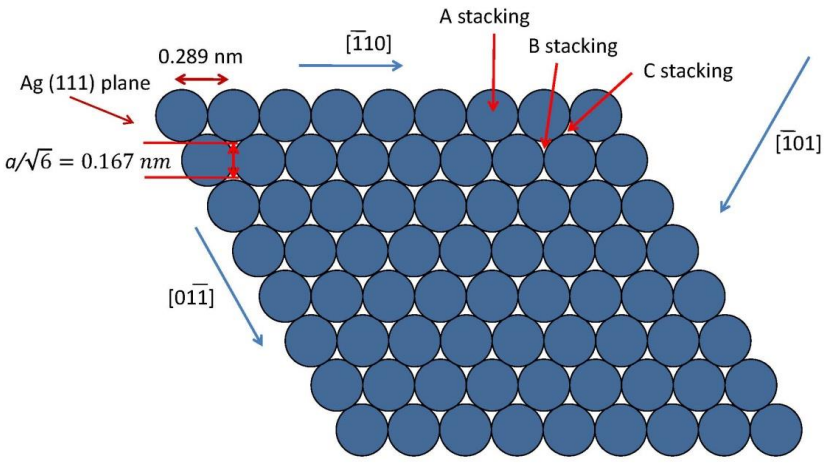

Approved for Public Release//Distribution Unlimited.

11

Graphite Basal Plane

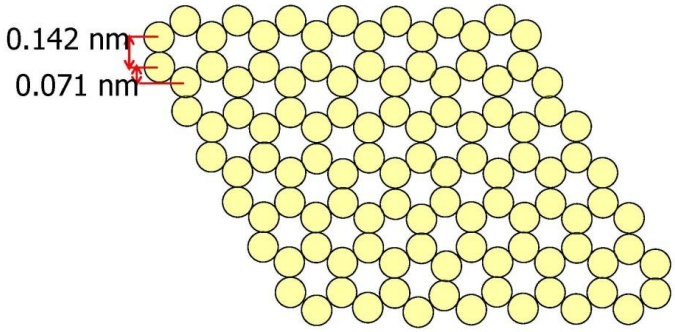

C-C interatomic distance ~ low potential site separation in Ag
0.142 nm ~ 0.167 nm (14.9% mismatch)

Approved for Public Release//Distribution Unlimited.

12

Ag and C Planes

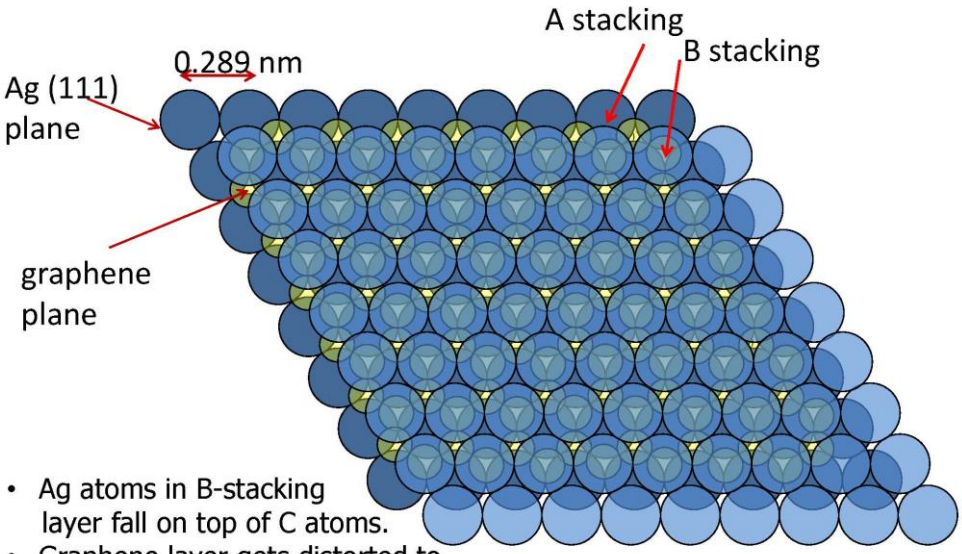

- Ag atoms in B-stacking layer fall on top of C atoms.
- Graphene layer gets distorted to accommodate stress.

Approved for Public Release//Distribution Unlimited.

13

DFT Simulation of Alternating Graphene and Ag(111) Layers

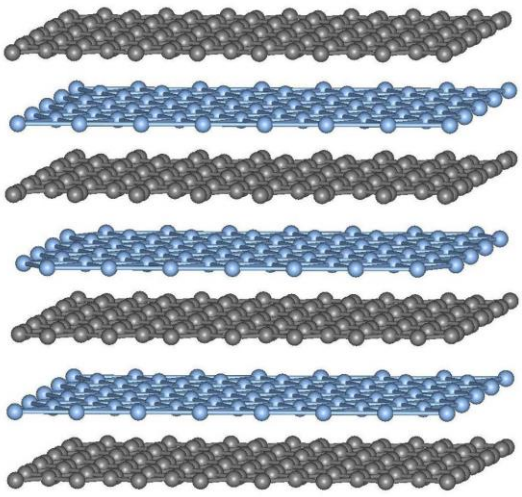

➢Calculations indicate that defect-free Ag and graphene layers do not form chemical bonds and do not "stick" to each other.

Approved for Public Release//Distribution Unlimited.

14

Two Vacancies per Supercell in Interfacial Graphene Layer on Ag(111) Surface

Side view

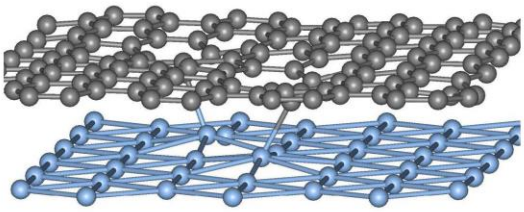

Top view

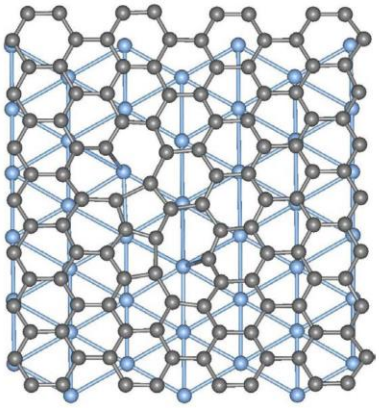

Binding Energy = 2.8 eV (1.4 eV per one vacancy)

➢**Only under-coordinated carbon atoms surrounding carbon vacancies in boundary graphene sheet have a chance to attach to Ag atoms on the Ag (111) surface**

15

Three Vacancies per Supercell in Interfacial Graphene Layer on Ag(111) Surface

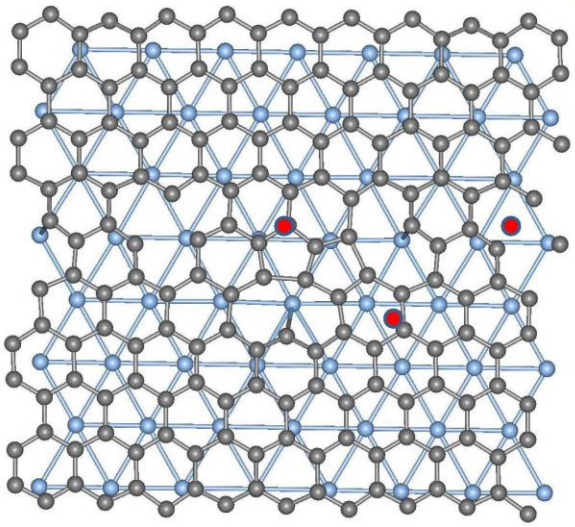

Top view

Binding Energy = 3.6 eV (1.2 eV per one vacancy)

➢**Only under-coordinated carbon atoms surrounding carbon vacancies in boundary graphene sheet have a chance to attach to Ag atoms at Ag (111) surface**

16

Several Rows of C Vacancies at Boundary Graphene Layer (Graphene Ribbons)

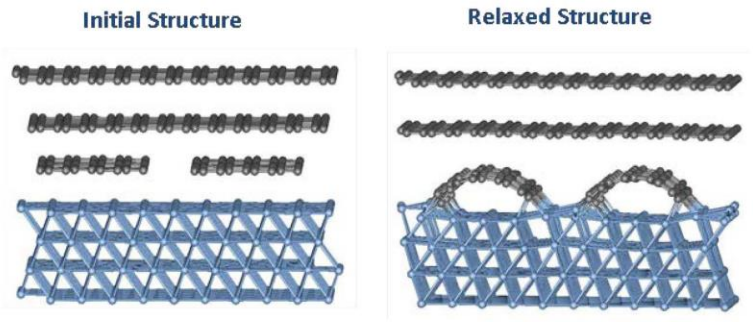

- Other structures (combined vacancy rows with single vacancies; defects at Ag surface, etc.) also show bonding between Ag and C.
- Bending of the graphene ribbon at the edges.

Two Rows of Vacancies per Supercell in Boundary Graphene Layer on Ag(111) Surface (graphene ribbons)

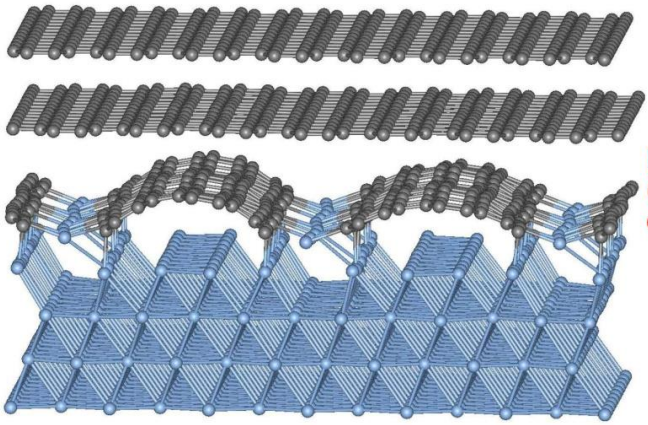

Binding Energy = 17 eV (1.4 eV per one "ribbon edge" atom)

- Only under-coordinated carbon atoms positioned along the edges of ribbons in boundary graphene sheet have a chance to attach to Ag atoms at Ag (111) surface
- Surface Ag atoms may leave the Ag surface and go to the edges of graphene ribbons, i.e., at the interface both Ag and C layers undergo serious reconstruction!

DFT: Graphene in Ag Covetic

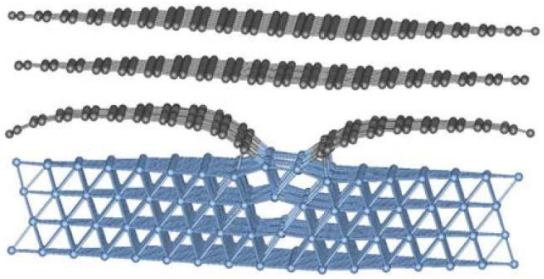

- Wider graphene ribbons have flatter surfaces.
- Bonding between Ag and C occurs at edges of ribbons.

Nature of Chemical Bonding Between Graphene Layer and Surface Ag Atoms

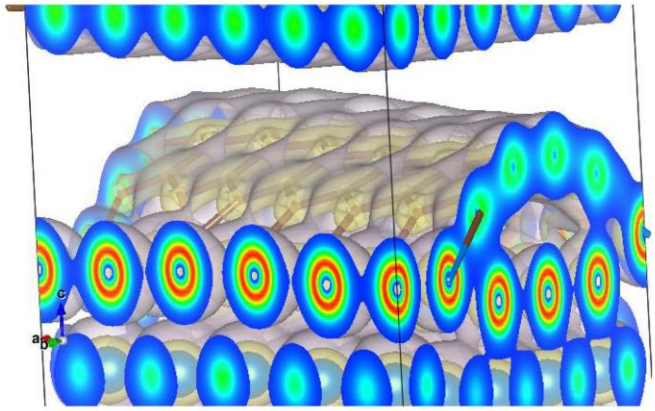

➢**Only under-coordinated carbon atoms positioned around vacancy and/or at the edges of graphene ribbons attach to Ag atoms.**

➢**Analysis indicates that C-Ag bond is a typical covalent bond (common electronic orbitals formation) similar to C-H bonds in hydrocarbons.**

Structure of Bulk Al Covetic

Al Alloys

As-extruded Al 6061
As-extruded Al 6061 cv 3% (6.5 at%)

Al 7075 cv 3% and 5% (10.57 at%)

Al 5083 cv 2% (4.37 at.%) with 0, 2.5, 5, 7.5, 10 and 15% cold rolling.

XRD from Al 7075 Covetic

0 % C

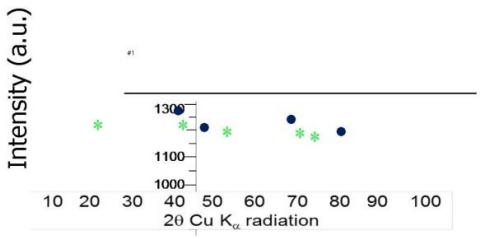

3 % C (6.5 at. %)

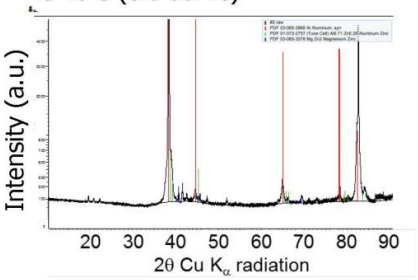

5 % C (10.57 at.%)

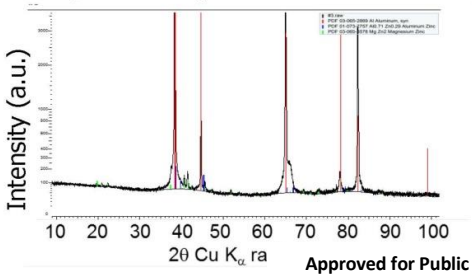

- Data for all three samples shows secondary phases: $Al_{71}Zn_{29}$ • and $MgZn_2$ * .
- No evidence of any carbon phase.

Secondary phases also found in other Al alloys.

C-K Map on SEM Image of Al 6061 cv 3% (6.5 at.%)

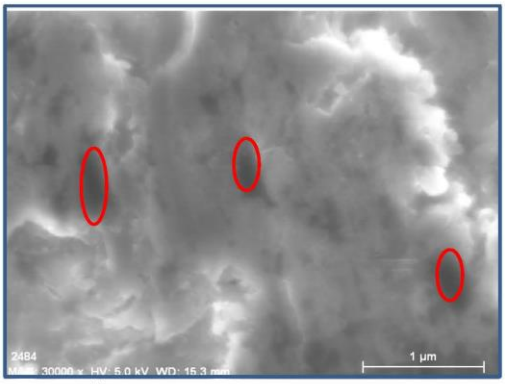

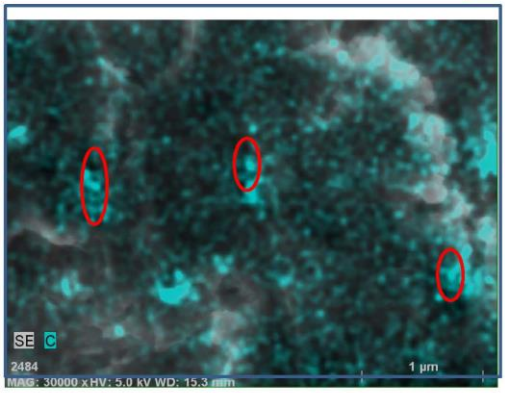

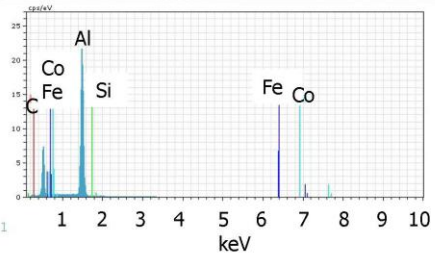

Carbon appears to form a network of chains connecting the larger particles

Evidence for "Graphite" in Al cv 3% (6.5 at. %)

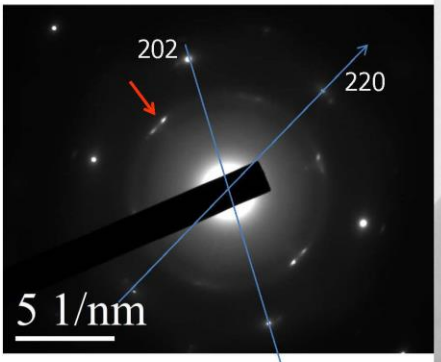

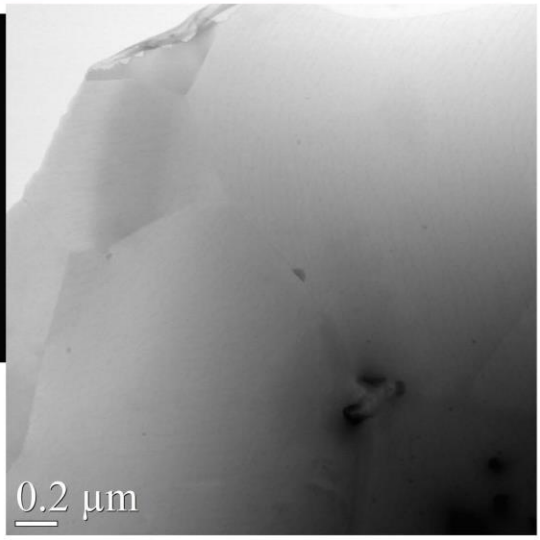

- Weak spots with arrows agree with graphite g-vectors for $[10\bar{1}0]$.
- DP Superposition of:
  $(1\bar{1}\bar{1})$ from Al and
  (0001) from graphite.

BF STEM image

BF/HAADF STEM Images of Stripes in Al 6061 cv 3%

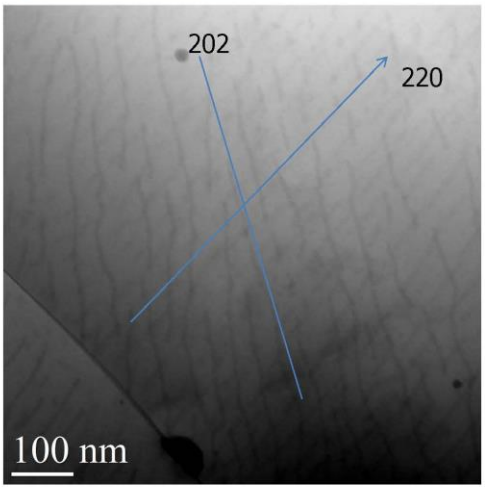

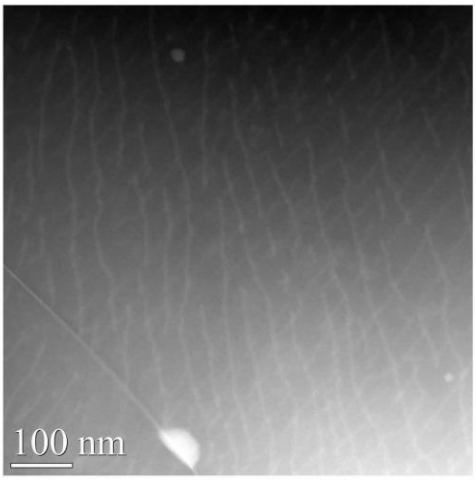

BF STEM Image

HAADF STEM Image

- Stripes close to the [220] and [202] directions of Al.
- Are the stripes dislocations?

Preferred Orientation of "Graphite" DP

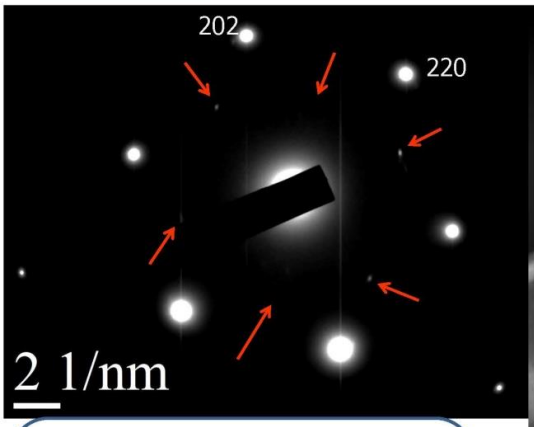

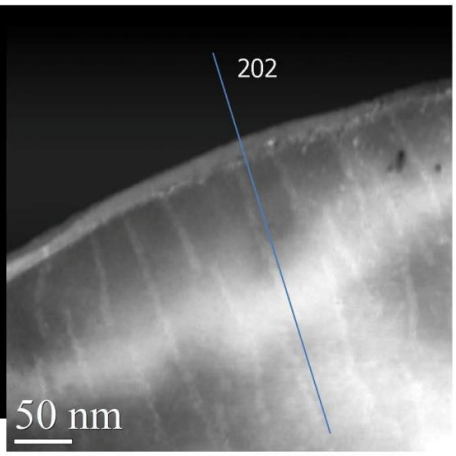

- Weak spots with arrows agree with graphite g-vectors for $[10\bar{1}0]$
- Preferentially align with Al spots
- DP Superposition of:
  $(1\bar{1}1)$ from Al and
  (0001) from graphite

- HAADF STEM image showing stripes close to the [202] direction of Al
- Are the stripes dislocations?

27

Stacking of "Graphite" on Al

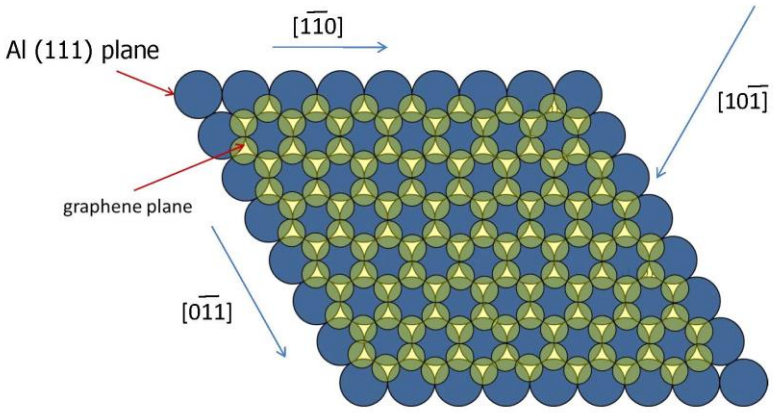

- Same crystalline orientation as in Ag covetic.
- There is a 13% mismatch between Al low potential sites and C-C distance in graphene.

28

C-K Edge EELS Spectrum Image Map from Al 6061 cv 3%

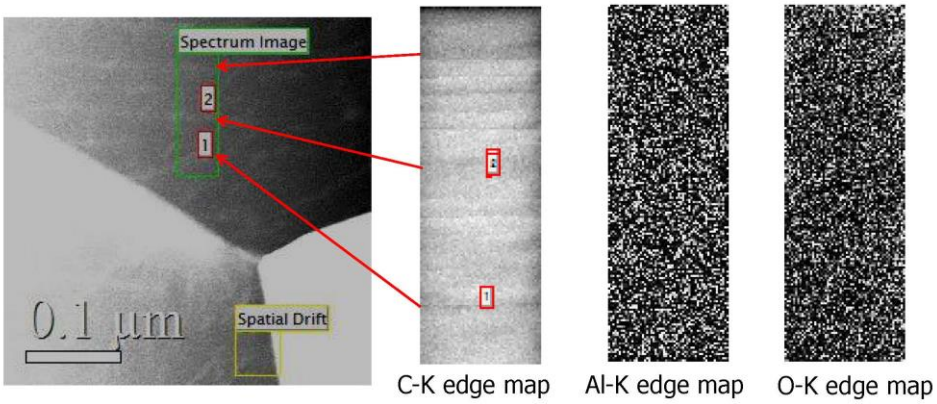

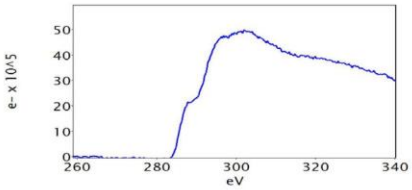

- Uniform Al and O content
- Slightly lower C content in stripes.

29

Approved for Public Release//Distribution Unlimited.

Model of the Stripes in Al 6061 Covetic

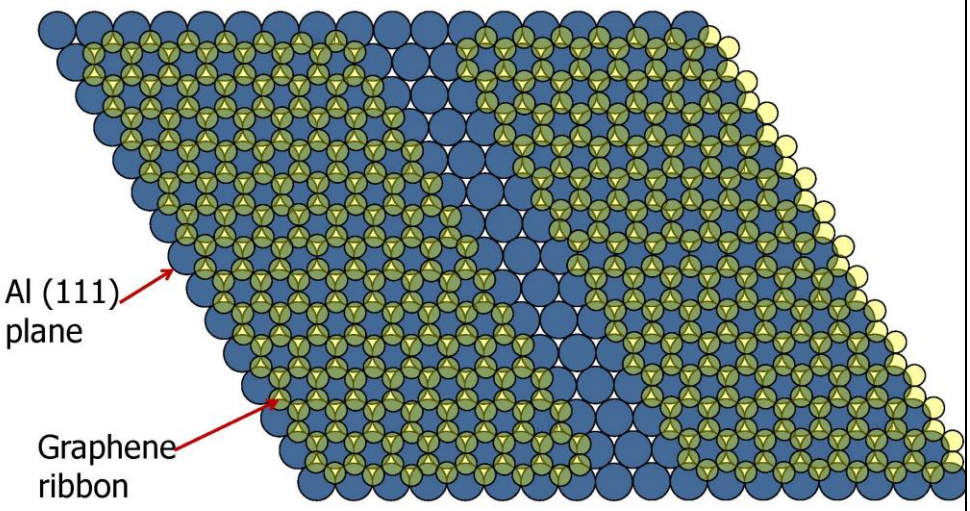

Carbon in Al covetic forms ribbons with edges parallel to <110> directions of Al.

30

Approved for Public Release//Distribution Unlimited.

DFT of Aluminum Covetic

AIC (side view)

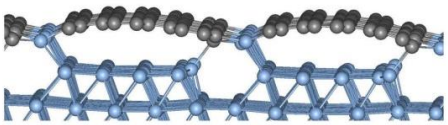

AIC (top view)

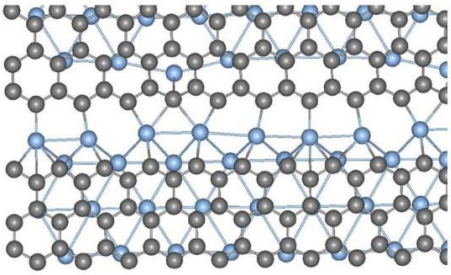

- Bonds between Al and C at edges of ribbon and vacancies in the graphene.
- Each C atom can bond to two or three Al atoms.
- Some Al atoms move to the graphene layer.

Structure of Bulk Cu Covetic

XRD of Bulk Cu Covetic

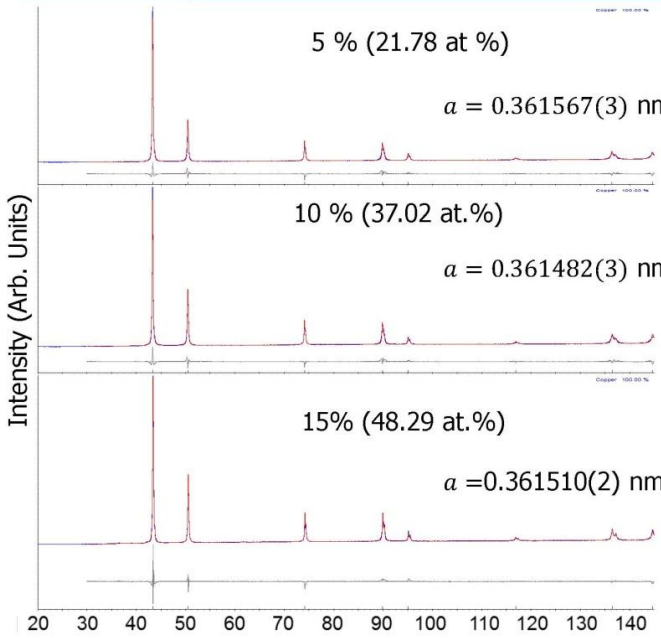

- No impurity phases or allotropes of C.
- Slight increase in lattice constant compared to bulk Cu a=0.36149 nm.
- Preferred orientation <111>
- or possibly a difference in structure?

33

Modulation in Copper Covetic at the Nanoscale

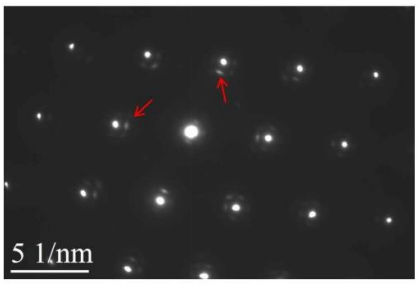

Cu cv 2% (9.75 at. %)

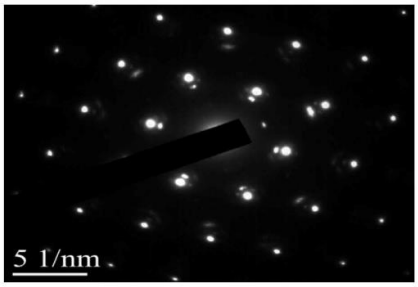

Cu cv 5% (21.78 at. %)

(110) Diffraction patterns.

Weak spots are observed corresponding to a modulation of ~1.6 nm.

The weak spots are stronger for the Cu cv 5% C.

What is the origin of the weak spots?

34

Modulation by HAADF and HRTEM

Cu cv 2% (9.75 at.%)

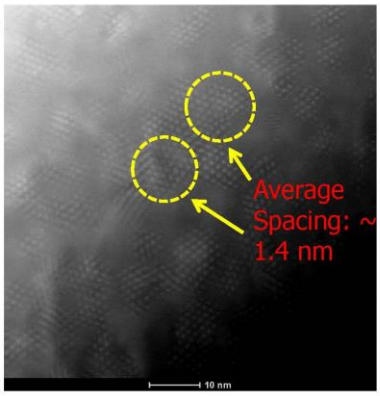

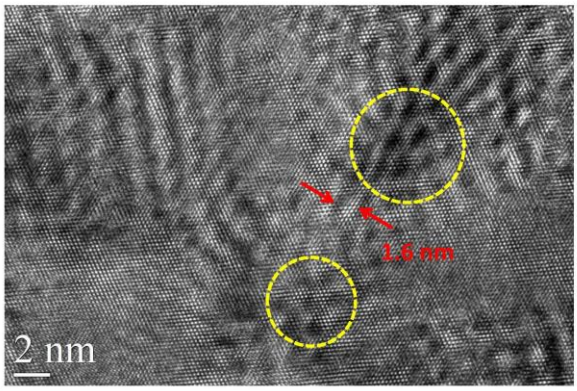

HAADF image
Obtained at NIST

HRTEM image

Modulation of ~1.6 nm along different crystallographic directions.

35

Cu cv 5% (21.78 at.%) EDS

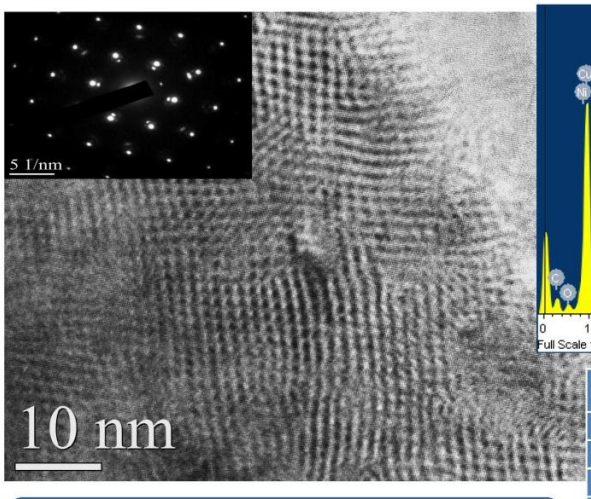

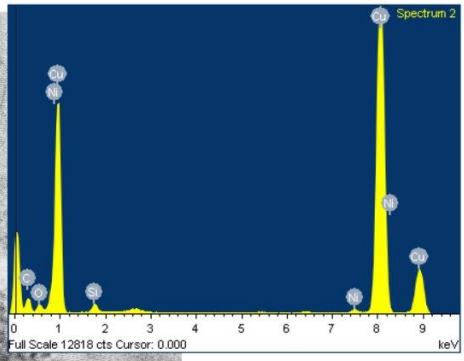

Element	Weight%	Atomic%
C K	7.44	28.25
O K	1.98	5.65
Si K	1.17	1.89
Ni K	0.84	0.65
Cu K	88.57	63.55
Totals	100.00	

Continuous network associated with region of high C content 7.4 wt % superimposed on Cu lattice planes.

36

Structure of Cu covetic

Lattice constant of fcc Cu a=0.3610 nm

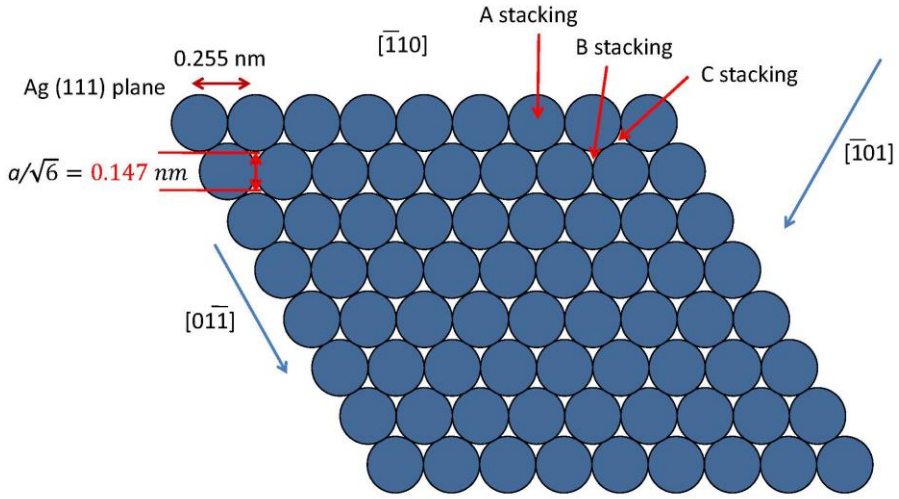

- C-C interatomic separation = 0.142 nm.
- Smaller mismatch between graphene and copper (111) ~ 3%.

37

Approved for Public Release//Distribution Unlimited.

Graphene on Cu (111)

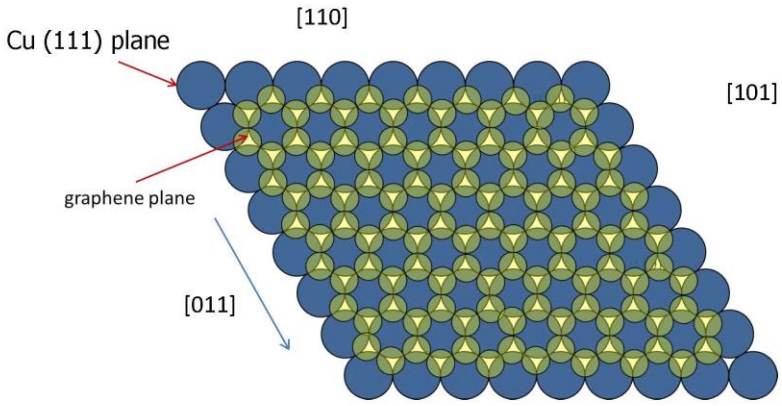

Better match between Cu (111) plane and graphene than Ag and Al.
However, Cu is a large atom:
r_{Cu} =128 pm, r_{Ag}= 144 pm, r_{Al} = 143 pm, compared to r_C=77 pm

Approved for Public Release//Distribution Unlimited.

38

Distances in the fcc Unit Cells of Ag, Al and Cu Covetics

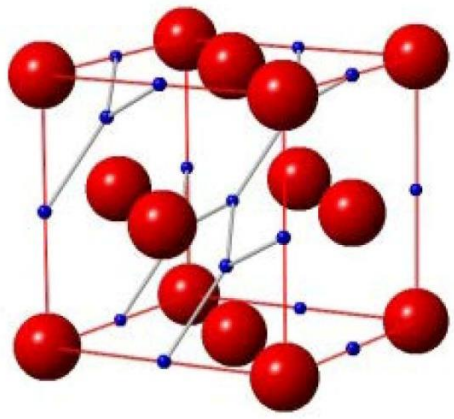

r_{Cu} =128 pm, r_{Ag}= 144 pm, r_{Al} = 143 pm

r_C=77 pm

$$d_{Ag-C} = \frac{a}{2} - r_{Ag} - r_C = -0.0165 \text{ nm}$$

$$d_{Al-C} = -0.0175 \text{ nm}$$

$$d_{Cu-C} = -0.0245 \text{ nm}$$

There is less space to accommodate C in Cu than in Ag or Al.

What is a model for the structure of Cu covetic?

Evidence of *sp2* Carbon in Covetics: Raman Scattering

Raman Scattering of Graphitic *sp2* Carbon

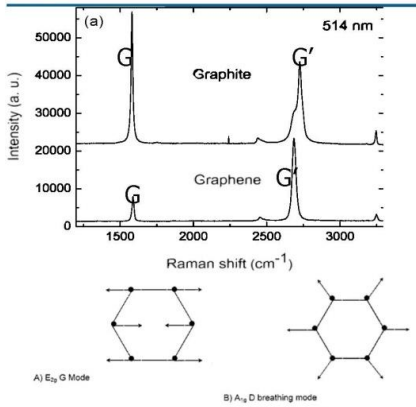

A.C. Ferrari, et al. PRL 97 , 187401 (2006).

Raman spectrum of SWCNT.
- Clear D peak in CNT.
- Radial Breathing Mode RBM

$$\omega_{RBM} = \frac{248}{d}\ \text{cm}^{-1}$$

d: nanotube radius

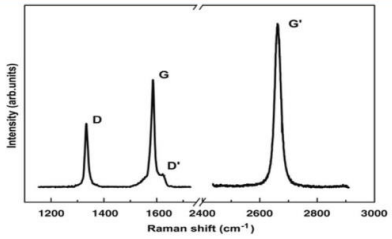

Raman spectrum from graphene edge shows D peak ($A_{1,g}$ breathing mode).
L.M. Malard, et al. Phys. Reports 473, 51 (2009).

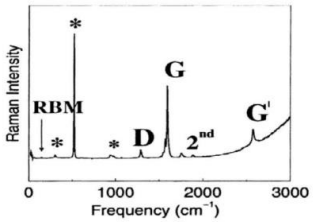

M.S. Dresselhaus, et al. Carbon 40, 2043 (2002).

41

Approved for Public Release//Distribution Unlimited.

Raman Scattering from Amorphous Carbon and Diamond (*sp3* bonding)

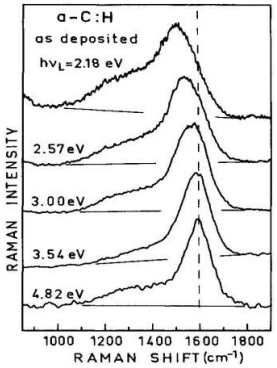

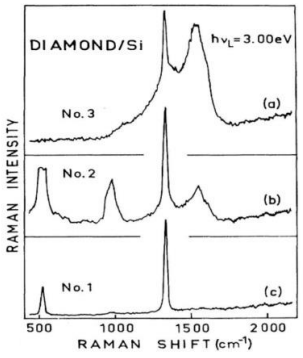

J. Wagner, et. al. Phys. Rev. B **40**, 1817 (1989).

- Raman spectra from amorphous C have broad peak around 1,600 cm^{-1}
- Raman spectra from diamond have strong peak at 1330 cm^{-1}

Approved for Public Release//Distribution Unlimited.

42

Raman Spectrum from Ag

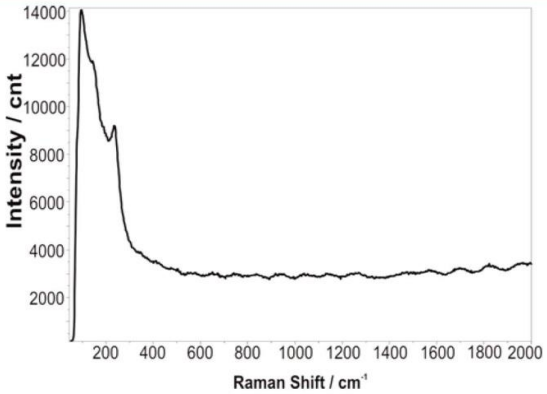

Irene Martina, et. al., e-Preservation Science 9, 1-8 (2012).

Peak at 95 cm^{-1} -- Ag lattice vibration modes
Peaks at 233, 345, 409 cm^{-1} -- Ag-Cl stretching modes

No peaks at 1,300 and 1,600 cm^{-1} in silver.

Approved for Public Release//Distribution Unlimited.

43

Raman Scattering from Ag covetic

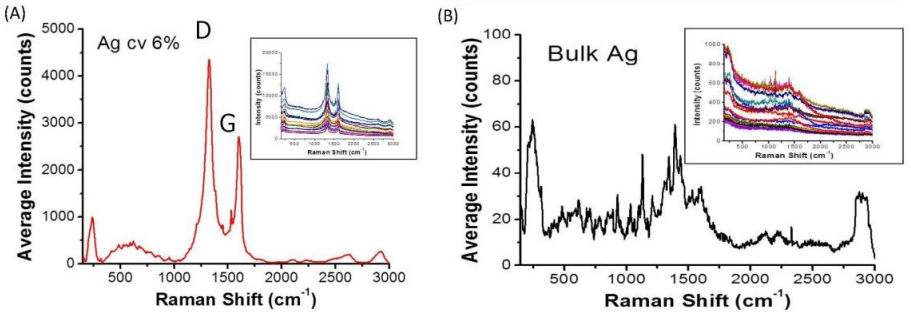

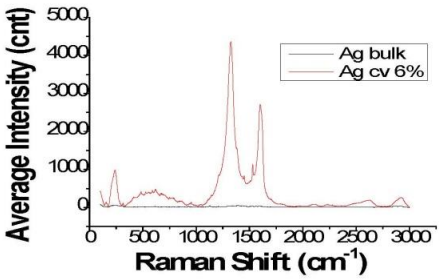

- Ag covetic shows clear D and G graphitic peaks at ~1,300 and 1,600 cm^{-1} in all 20 points of the sample.
- Ag metal shows weak signal in this region in all 20 points.
- The signal for Ag metal is much weaker than for Ag covetic.

sp2 graphitic carbon forms in Ag covetic.

44

Approved for Public Release//Distribution Unlimited.

Raman Mapping of Ag cv 6%

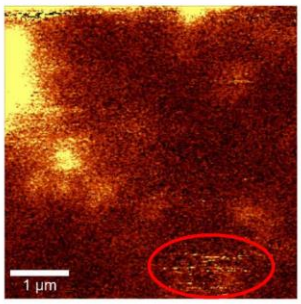

Raman map of D peak (1290-1390 cm^{-1})

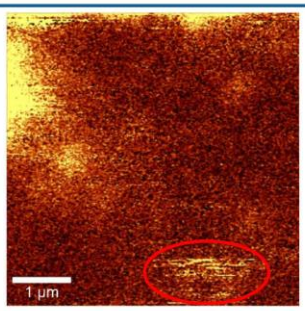

Raman map of G peak (1570-1650 cm^{-1})

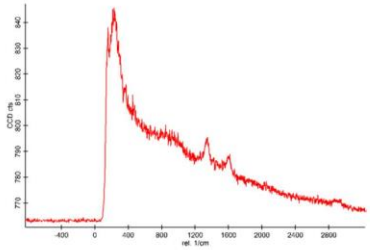

Single spectrum

- Distribution of C is not uniform on the sample.
- Domains of ~ 0.5 microns.
- Apparent formation of carbon ribbons in the sample. Possibly graphene?

Data obtained by Chen Gong at UMD

45

Approved for Public Release//Distribution Unlimited.

Raman Scattering of as-extruded Al 6061 Metal and Covetic

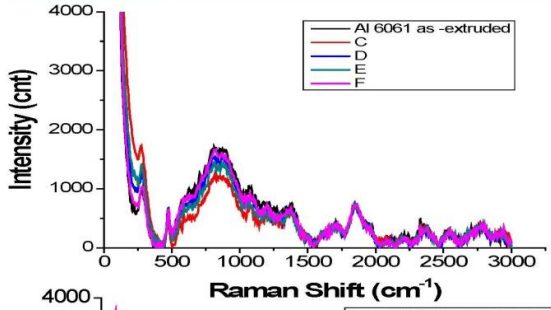

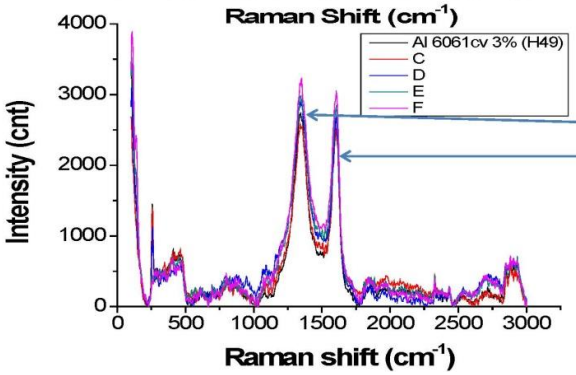

- Spectra from Al 6061 metal shows weak signal with a broad peak (500-1000 cm^{-1}).
- No evidence of D and G peaks from *sp2* carbon.
- Spectra from Al 6061 cv 3% shows strong and clear D and G peaks of graphitic C from all points.
- A broad peak (250-500 cm^{-1}) is observed.

46

Approved for Public Release//Distribution Unlimited.

Al 6061 after T6 Treatment

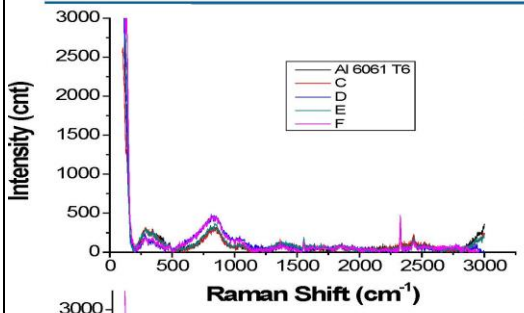

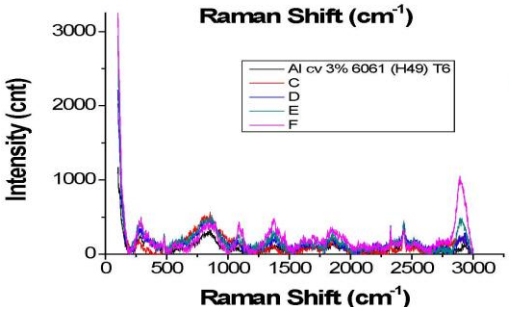

- Still no sign of graphitic carbon in As-extruded Al 6061 T6.
- Graphitic signals at 1,300 and 1,600 cm^{-1} are greatly reduced after T6 treatment.
- What is the cause of this decrease?

47

Al 7075 cv 3%

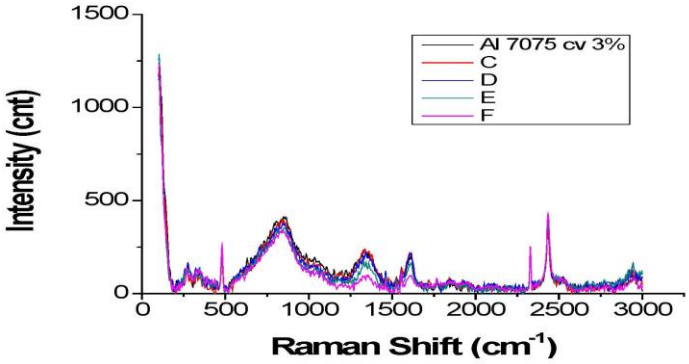

- Al 7075 cv 3% also shows strong broad peak 500 – 1000 cm^{-1}.
- D and G peaks from *sp2* graphitic carbon are also observed in all points.
- Weak peaks from 250-500 cm^{-1}.
- Overall intensity is weaker than Al 6061 cv 3%.

48

Al 5083 cv 2 % vs. % Cold Rolling

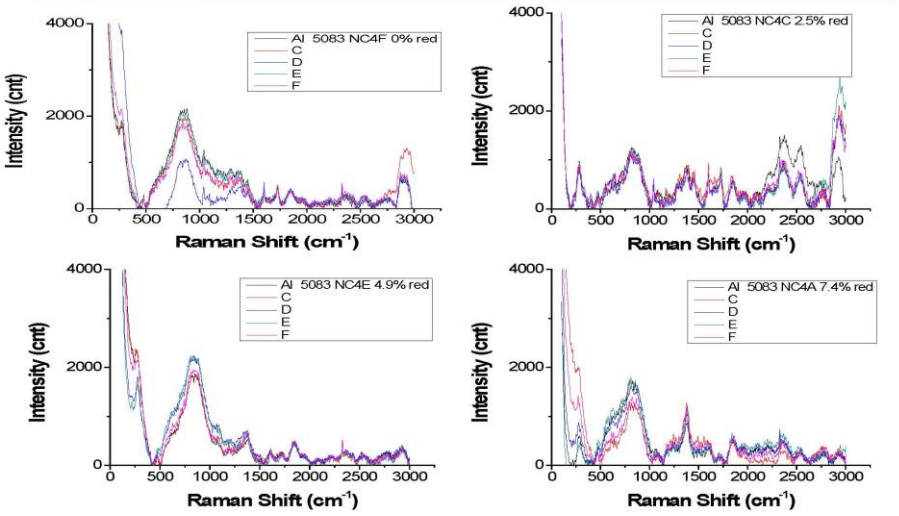

- This series of Al 5083 covetics also shows the D and G peaks at ~1,300 and 1,600 cm^{-1} for graphitic *sp2* carbon.
- Weaker signal than for Ag or Al 6061.

49

Al 5083 cv 2%

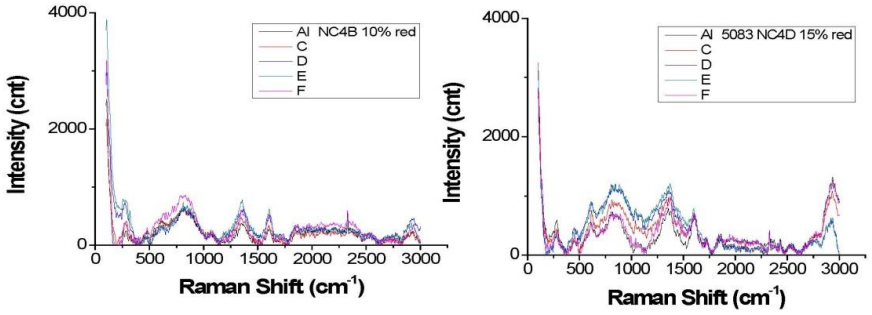

- Al 5083 covetics samples with higher % cold rolling show better defined D and G peaks but not as clear as Al 6061 covetic.
- There is no strong dependence on % of cold rolling.
- D and G peaks are better defined at higher % of cold rolling.

50

Phonon Density of States in Ag covetic: Model Structure

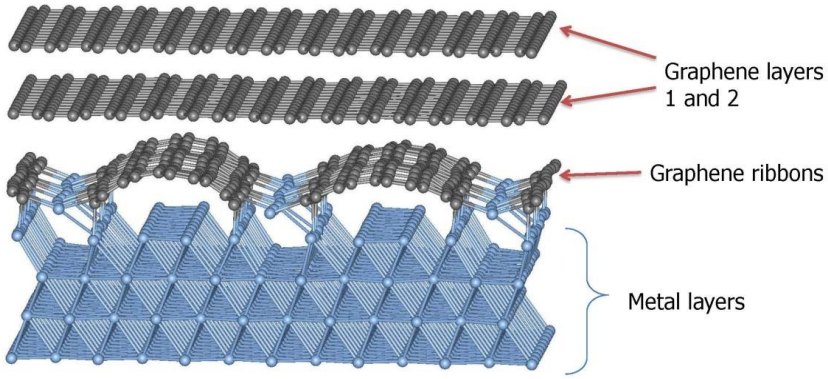

Phonon density of states was calculated for structures with 2, 1 or zero graphene layers over the layer with graphene ribbons in the supercell.

51

Phonon Density of States for Ag cv

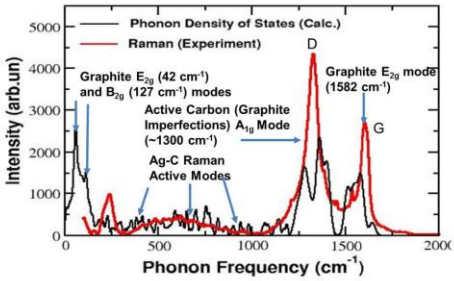

(2 Graphene Planes in Supercell)

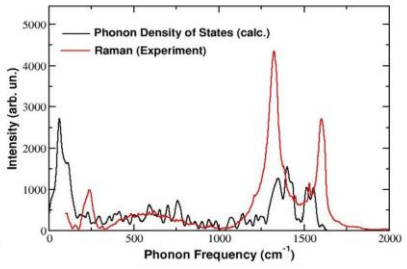

(1 Graphene Plane in Supercell)

Phonon density of states agrees with Raman spectrum.

- D and G peaks are reproduced for 2 graphene planes
- The intensity of the D and G peaks in the phonon density of states decreases with 1 graphene layer.
- Broad peak 300-1,000 cm^{-1} is due to Ag-C modes.

52

Phonon Density of States of Al Covetic

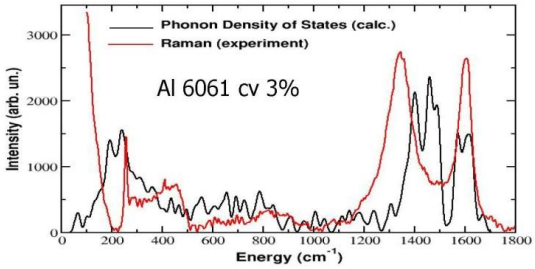

- Al 6061 cv 3% better fit for two graphene layers

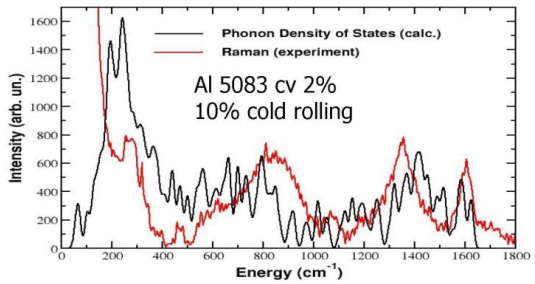

Al 5083 cv 2% better fit for zero graphene layers

53

Approved for Public Release//Distribution Unlimited.

Phonon Density of States for Cu cv 10%

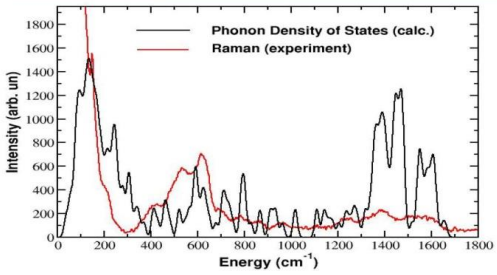

Phonon density of states with one graphene layer.

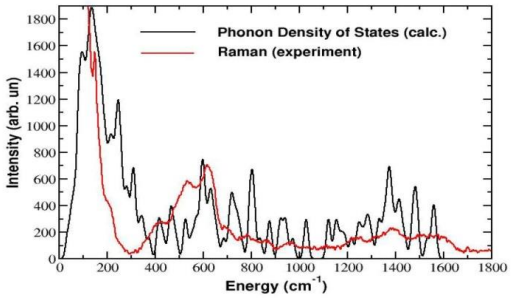

Phonon density of states with zero graphene layers

Best fit to Raman data for zero graphene layers.

54

Approved for Public Release//Distribution Unlimited.

Evidence of sp2 bonding in Covetics: EELS

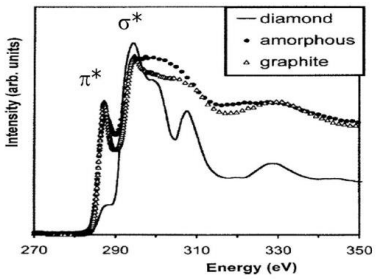

L. Nistor, et al., Phys. Stat. Sol. **186** 207-14 (2001).

C-K edge:

- Feature at 284 eV corresponding to excitation of 1s electron to π* antibonding unoccupied orbital.
- Feature at ~290 eV corresponds to transitions to σ* state.
- Clear difference in the signal from carbon with different bonding (*sp2* or *sp3*).

Approved for Public Release//Distribution Unlimited.

55

Comparison of EELS C-K Edge Spectra

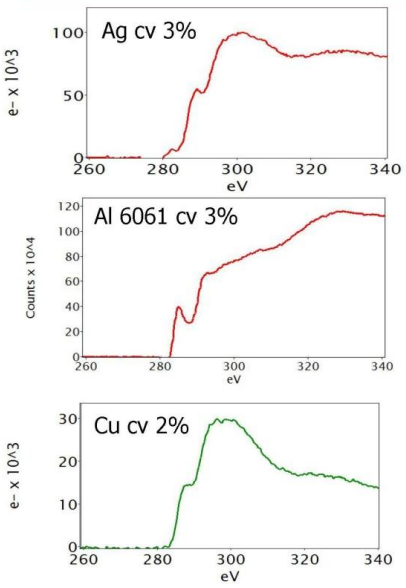

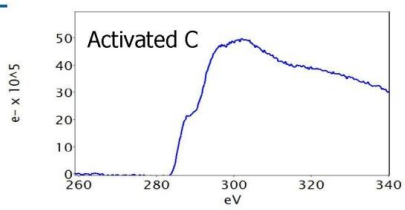

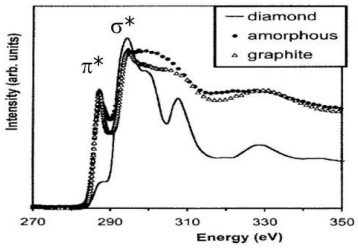

L. Nistor, et al., Phys. Stat. Sol. **186** 207-14 (2001).

Covetics show similar *sp2* signal as activated C source and *sp2* bonded C.

56

Approved for Public Release//Distribution Unlimited.

Electrical Properties of Ag Covetic

Electrical Properties of Ag covetic

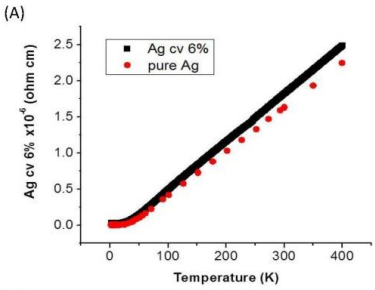

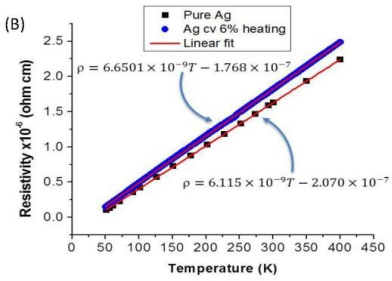

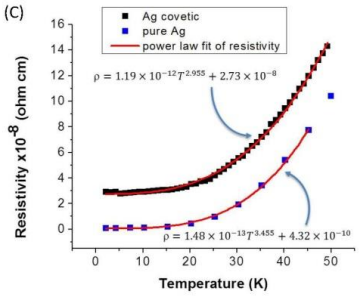

- Resistivity of Ag cv 6% shows similar temp. dep. of resistivity to Ag but with higher slope.
  - Stronger electron-phonon interaction in Ag covetic compared to Ag metal.
- Low temp range has smaller exponent 2.96 vs 3.45 for Ag metal.

Temperature Dep. of Resistivity of Metals

Bloch-Grüneisen Formula for the resistivity of a pure metal

$$\rho(T) = \rho_o + \underbrace{\frac{C}{M\theta}\left(\frac{T}{\theta}\right)^5 \int_0^{\theta/T} \frac{z^5 e^z}{(e^z-1)^2} dz}_{\rho_i(T)}$$

$\rho_i(T) \rightarrow 124.431 \frac{C}{M\theta}\left(\frac{T}{\theta}\right)^5$ as T→0

$\rho_i(T) \rightarrow \frac{C}{4M\theta}\left(\frac{T}{\theta}\right)$ as T→∞

C: constant of the metal,
T: temperature
θ: characteristic temp. "electrical resistivity Debye Temp."
M: atomic weight

Cu Covetic Thin Films

Deposition of Cu Covetic Films

e-beam deposition

- Base pressure $5x10^{-6}$ Torr
- voltage of 8 kV and current of 90-130 mA
- Target: Cu cv 5%, 10% and 15%
- Substrate: Si (001) and glass
- Substrate temp: 25 °C and 350 °C
- Thickness 10-200 nm

PLD deposition

- PLD: Quantel Brilliant B solid-state system
- Nd:YAG pulsed laser (400mJ/pulse @ 532nm, 10Hz)
- Power 1.88-3.2 Watts
- Pressure: 10^{-2}-2 Torr, Nitrogen and Ar gas
- Substrate Temp: 150, 350 °C
- Target: Cu cv 4%
- Target prep: 1 min ablation

e-Beam Films

Analysis of e-beam Cu cv 5% Film on Si

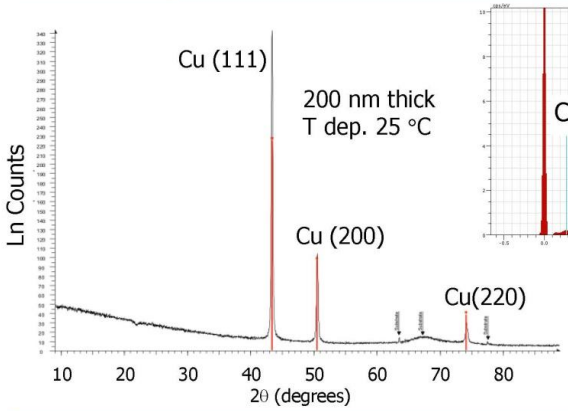

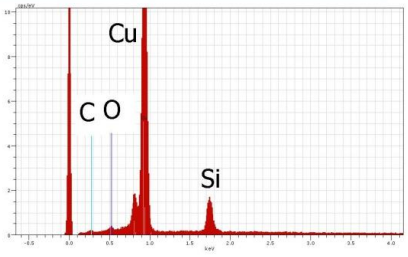

Element	Weight %	Atomic %
Cu	97.47	89.25
C	1.29	6.23
O	1.24	4.52

- Cu covetic film is highly crystalline. Preferred <111> orientation.
- No Copper oxide phases are observed.
- No C phases in the XRD pattern.
- C is transferred to the film.
- C incorporation in the film is lower than the target used for deposition.

63

Low Mag. TEM Image and DP of e-beam Deposited Cu cv 5% Film (Tdep. 25 °C)

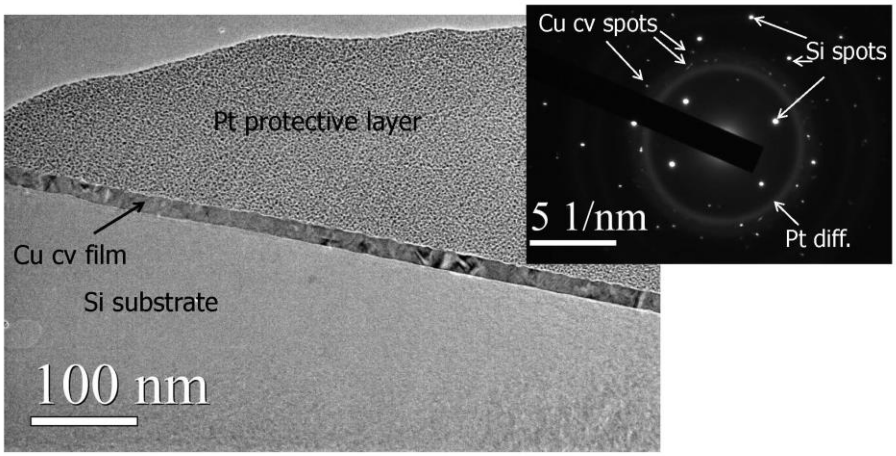

- The Cu cv film is very continuous with fairly flat surface through the whole TEM sample ~ 5 microns.
- The DP shows strong spots from Si substrate, weak spots from Cu cv film and broad ring from Pt protective layer.

64

Thickness of Cu cv Film

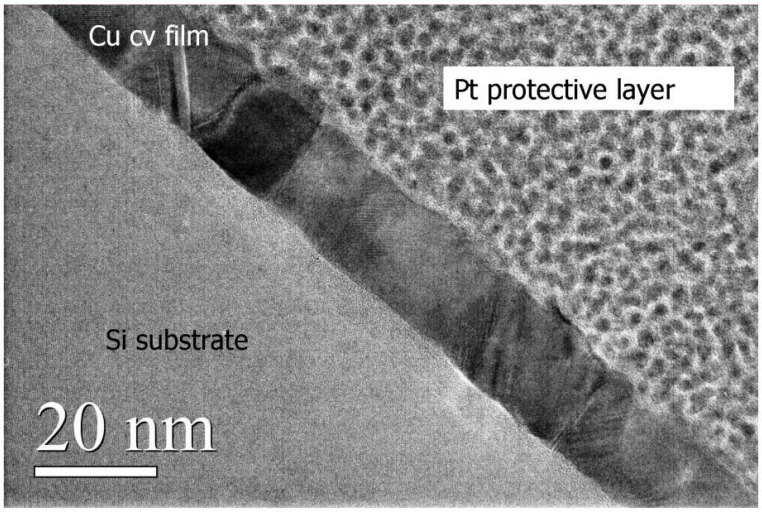

At higher magnification we see slight roughness of the film surface and polycrystallinity of the film with columnar structure.

Cu cv 5% Film Thickness

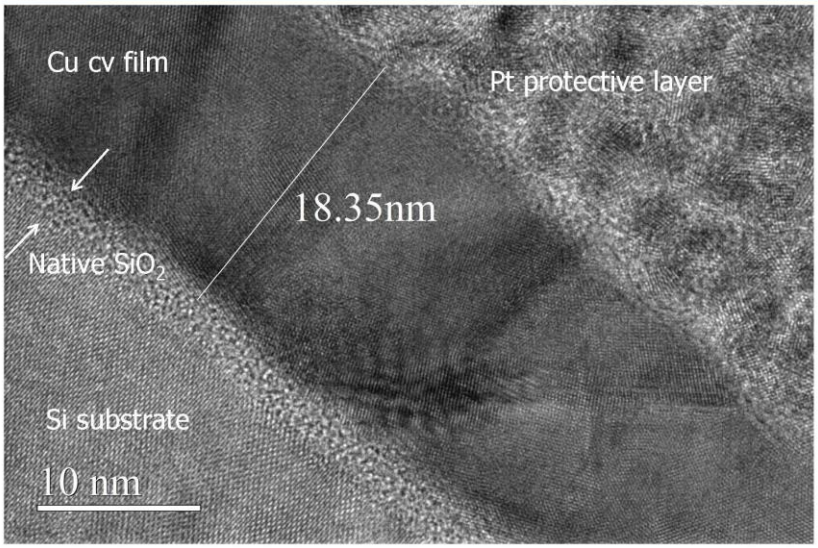

Film thickness fairly regular. Grains extend from SiO_2 to film surface.

Transmittance of Cu cv 5% and Cu Films Grown at 25 °C on Glass

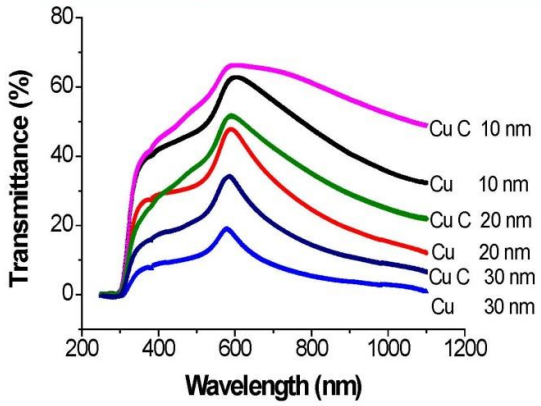

- Cu covetic films are more transparent than Cu metal films of the same thickness.
- How transparent are films with higher C content?

Resistivity of Cu cv 5% Grown at 25°C

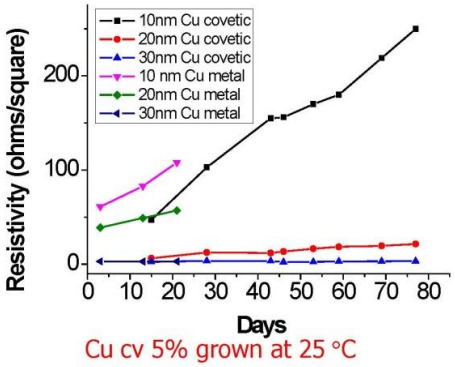

Cu cv 5% grown at 25 °C

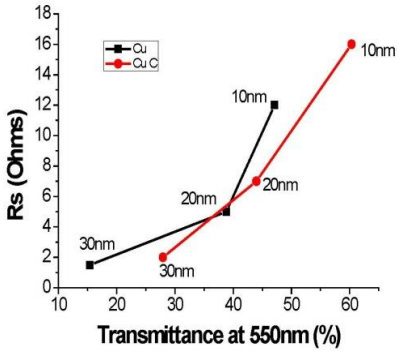

- Cu covetic films are more stable than copper films.
- Thinner films are more transparent but the resistivity changes faster with time than for thicker films.
- Need to get a material with T ≥ 90% and Rs = 10 ohm/square for transparent electrodes.

A paper to be submitted to Appl. Phys. Lett. is in preparation.

ITO is the Technology Standard for Transparent and Conductive Electrodes

Indium Tin Oxide

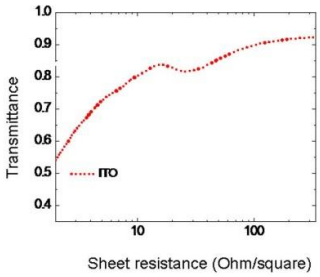

- Performance
- Cost of Indium
- Sputtering: high cost
- Brittleness when bent

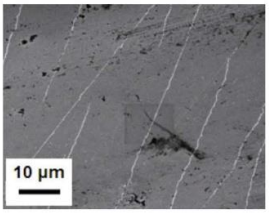

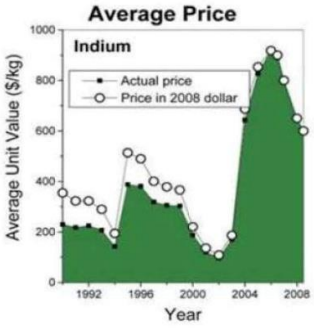

Other competing technologies use graphene and CNT and Ag or Cu nanowires.

69

Approved for Public Release//Distribution Unlimited.

Resistivity Data vs Time for Cu cv 15% Films

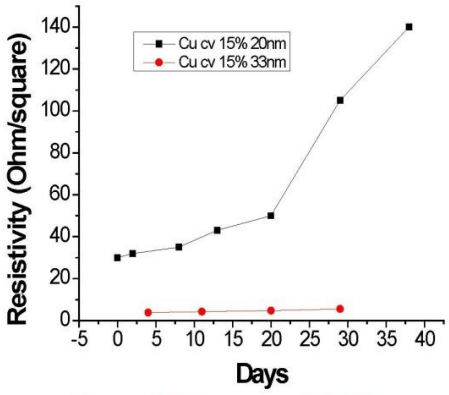

Cu cv 15% grown at 25 °C

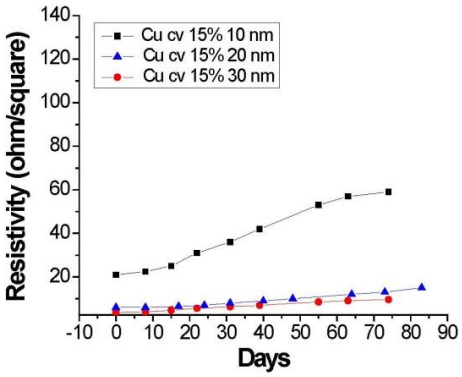

Cu cv 15% grown at 350 °C

Films grown at high temperature have better stability than films grown at room temperature.

Approved for Public Release//Distribution Unlimited.

70

Comparison of Film Thickness and C Content

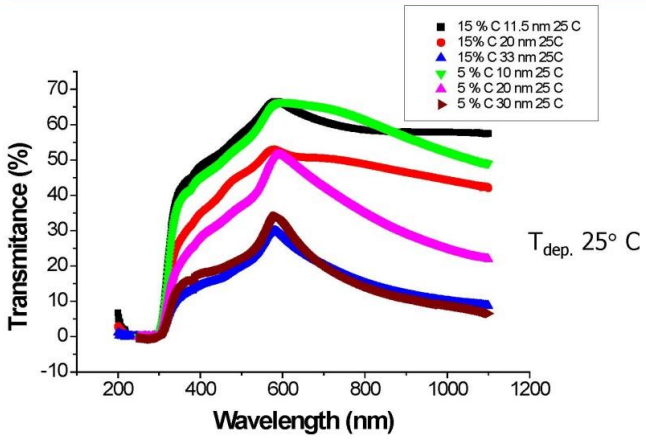

- Transmittance increases slightly with increasing C content.
- Slightly flatter transmittance curves for 15% C.
- What is the C content in the films?
- How does C change the energy band diagrams in covetics?

Transmittance of Cu cv 15% with Growth Temp.

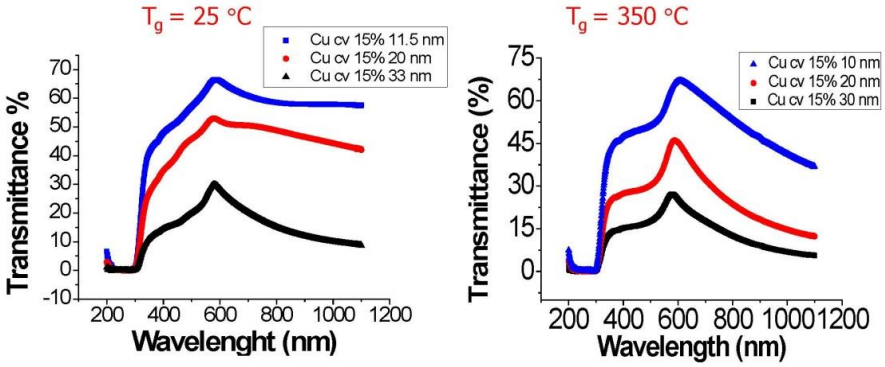

Transmittance has different shape for films grown at room temperature than at 350 °C.

- Films grown at 25° C have flatter curves.
- Films grown at 350° C have better defined peak at ~550 nm.

How Does C Affect the Energy Band Diagram of Copper?

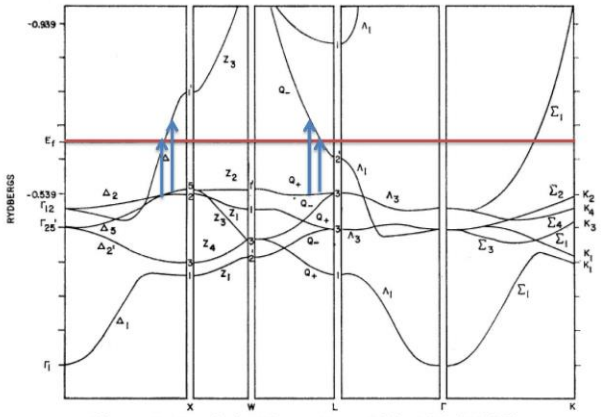

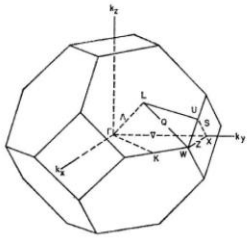

Brilloun zone of fcc crystals.

Glenn A. Burdick, Phys., Rev. 129, 138 (1963).

- Does C act as a "dopant" in Cu increasing the density of electrons in CB? This would increase conductivity and raise the Fermi level E_F.
- A higher E_F would give rise to more transmission of light to higher energies.

PLD of Cu cv Films

Sample Deposition Specification

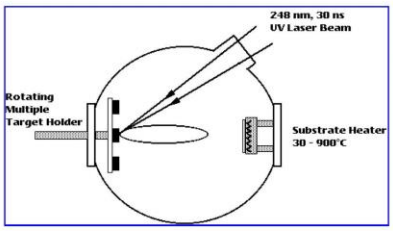

Advantages:
- Simple, flexible
- Multiple target possible
- Congruent evaporation
- Fast response
- Energetic evaporants

Disadvantages:
- micron-sized particles
- narrow forward angular distribution

Date Grown	06/12//14	07/09/14	07/11/14	07/30/14	08/29/14	09/18/14
Substrate	Si (100)	Si (100)	Si (100)	Si (100)	Si (100)	Si (100)
Laser Power (W)	1.93	1.8	3.55	3.3	3.2	3.2
Pressure (Torr)	1.00E-01	1.8	1.10E-01	1.00E-01	1.00E-01	9.50E-02
Substrate Temp. (°C)	150	150	150	350	350	150
Deposition time (mins)	15	15	21	64	64	60
Approx. Thickness (nm)	9.52	2.73	11.28	20.17	13.53	12.95
C content - EDS (%wt)				0.42	5.04	3.23

Film thickness estimated from n&k assuming values for Cu.

XRD from Cu cv PLD Film

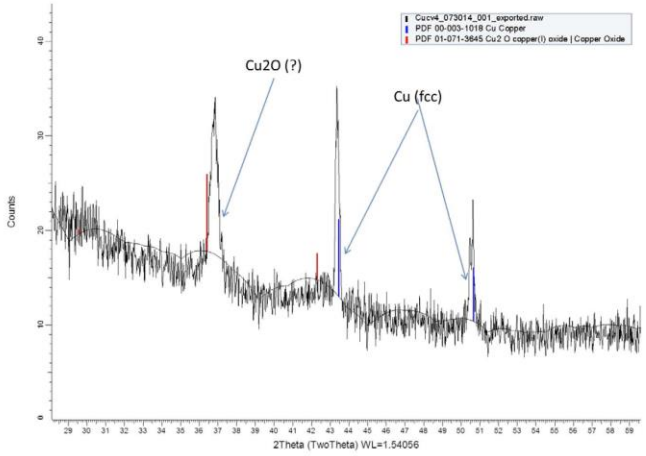

High Temp. high laser power shows mixture of Cu and Cu_2O/CuO

XRD Analysis of PLD Cu cv 4% Film

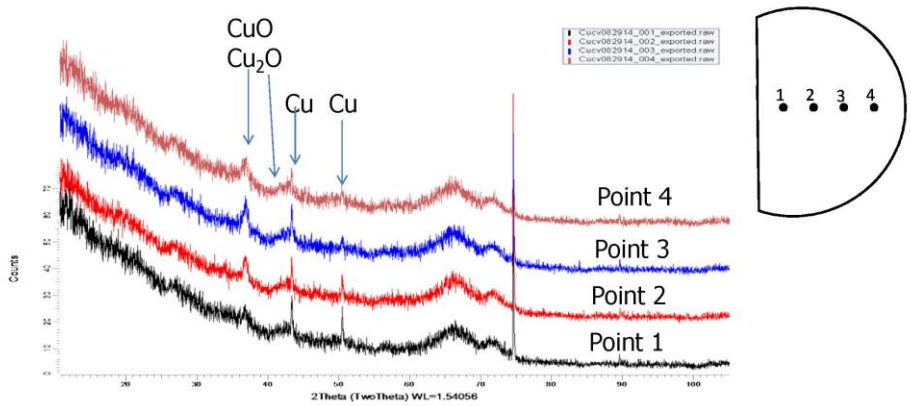

- PLD film has Cu and some CuO/Cu_2O.
- The peaks from Cu are stronger in position 1 of the sample.
- Used this position to grow another film.
- Average C 5.04 wt% by EDS. Higher than for e-beam films.

Optical Properties of PLD Cu cv Films

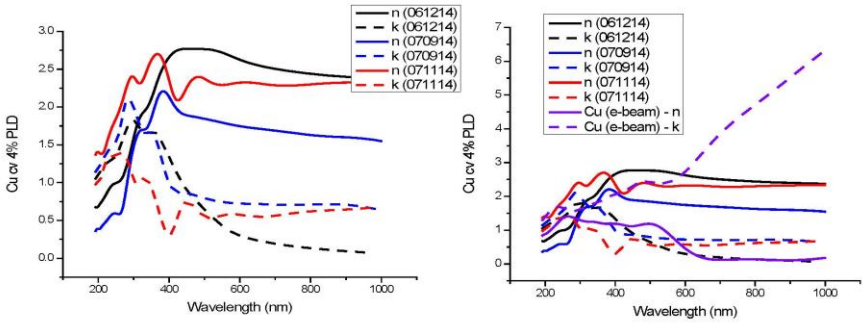

Wide variation in n, k depending on growth parameters.

- Low power, low pressure more like Cu_2O (black lines)
- Low power, high pressure maxima shifts to lower wavelength (blue lines)
- High power, low pressure signal closer to Cu. (red lines)
  - XRD showed mostly Cu_2O and/or CuO phases in these samples.

e-beam deposited films have n, k like pure Cu in agreement with XPS results from Azzam Mansour that C content is very small.

Optical Constants of Cu, CuO and Cu_2O

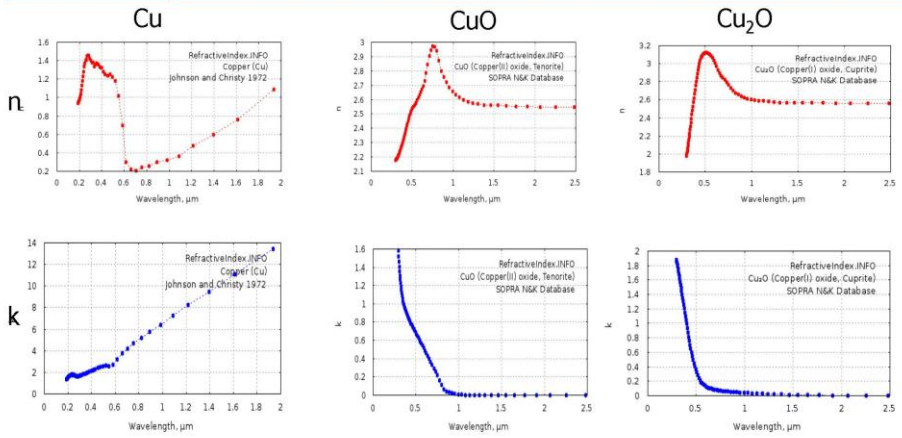

Cu and Copper oxides have very different optical properties

http://refractiveindex.info/legacy/?group=METALS&material=Copper&option=Johnson&wavelength=1.378E-4
http://refractiveindex.info/legacy/?group=CRYSTALS&material=CuO
http://refractiveindex.info/legacy/?group=CRYSTALS&material=Cu2O

79

Approved for Public Release//Distribution Unlimited.

Ellipsometry Raw Data From PLD Films

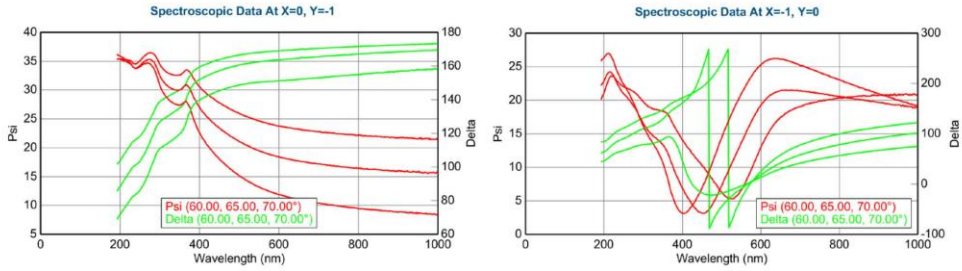

Cu cv 4% PLD (061214)

Cu cv 4% PLD (091814)

- Raw data for Psi and Delta for first set of films closer to Cu_2O and CuO
- Raw data for Psi and Delta for last set of films cannot be fitted to Cu_2O, CuO or Cu.
  - There is something different in these films. These are covetics.

Approved for Public Release//Distribution Unlimited.

80

Transmittance of PLD Cu cv 4% Film

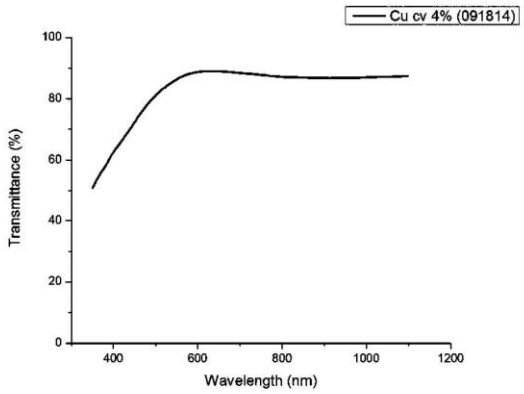

- 10 nm film, 3.23 % C by EDS
- Electrical resistivity too high in this film (film seems not to be continuous)

PLD seems to be a promising film deposition technique to transfer the carbon in covetics, but more work is necessary.

Conclusions

- Carbon in Ag and Al covetic forms ribbons or layers of *sp2* bonded carbon with a 3D epitaxial relationship with the Ag lattice.
  - Evidence of 3D epitaxy from TEM
  - Evidence of *sp2* bonding from Raman and EELS
- Covalent bonding between C and Ag or Al is predicted from DFT at edges of ribbons and C vacancies.
- Phonon density of states predicts M-C (M= Ag, Al and Cu) vibrational modes observed in Raman spectra of Ag and Al covetics.
- T6 treatment decreased the Raman signal of *sp2* C in Al 6061 covetic.
- Cu covetic shows different structure than Ag and Al covetic. A modulated structure is characteristic of regions containing high C content.
- Ag covetic shows stronger dependence of resistivity with temperature than Ag metal.
- PLD of Cu covetic films produced films with higher C content than e-beam films.
- Cu covetic films are more transparent than Cu films of same thickness
- Cu covetic films show higher environmental stability than Cu films

Papers in preparation.

1. L. Salamanca-Riba, et. al., "Three Dimensional Epitaxy of Carbon Nanostructures in Silver," to be submitted to Adv. Functional Materials.
2. R. Isaacs, et. al., "Nanocarbon-Copper Thin Film as Transparent Electrode," to be submitted to Appl. Phys. Lett.

www.darpa.mil

Approved for Public Release//Distribution Unlimited.

Thank you

Approved for Public Release//Distribution Unlimited.

INTENTIONALLY LEFT BLANK.

Lists of Symbols, Abbreviations, and Acronyms

Al	aluminum
Ag	silver
C	carbon
Cu	copper
DFT	discrete Fourier transform
EELS	electron energy loss spectroscopy
PLD	pulsed laser deposition
TEM	transmission electron microscopy
XRD	X-ray diffraction

1 (PDF)	DEFENSE TECHNICAL INFORMATION CTR DTIC OCA
2 (PDF)	DIRECTOR US ARMY RESEARCH LAB RDRL CIO LL IMAL HRA MAIL & RECORDS MGMT
1 (PDF)	GOVT PRINTG OFC A MALHOTRA
1 (PDF)	DIR USARL RDRL WMM F K DOHERTY